# On the Analysis of Data Emerging in Non-linear and Complex Systems

## Comparison of two X-ray Prony spectra

**RAUL R. NIGMATULLIN[1]*, A.S. KHRAMOV[2], A.G. KIYAMOV[2], B. F. FATKHULLIN[2] , J.T. MACHADO[3], DUMITRU BALEANU[4,5]**

[1] Kazan National Research Technical University (KNRTU-KAI), 10 Karl Marx Str., 420011, Kazan, Tatarstan, Russia

[2] Institute of Physics, Kazan Federal University, Kremlevskaya Str.,18, 420008. Kazan, Tatarstan, Russian Federation

[3] ISEP-Institute of Engineering, Polytechnic of Porto Department of Electrical Engineering, Rua Dr. Antonio Bernardino de Almeida, 431. 4200-072 Porto, Portugal

[4] Cankaya University, Department of Mathematics and Computer Sciences,Balgat 06530,Ankara, Turkey

[5] Institute of Space Sciences, Magurele, 077125, Romania

*New arguments proving that successive (repeated) measurements have a memory and actually remember each other are presented. The recognition of this peculiarity can change essentially the existing paradigm associated with conventional observation in behavior of different complex systems and lead towards the application of an intermediate model (IM). This IM can provide a very accurate fit of the measured data in terms of the Prony's decomposition. This decomposition, in turn, contains a small set of the fitting parameters relatively to the number of initial data points and allows comparing the measured data in cases where the "best fit" model based on some specific physical principles is absent. As an example, we consider two X-ray diffractometers (defined in paper as A- ("cheap") and B- ("expensive") that are used after their proper calibration for the measuring of the same substance (corundum $\alpha$-$Al_2O_3$). The amplitude-frequency response (AFR) obtained in the frame of the Prony's decomposition can be used for comparison of the spectra recorded from (A) and (B) – X-ray diffractometers (XRDs) for calibration and other practical purposes. We prove also that the Fourier decomposition can be adapted to "ideal" experiment without memory while the Prony's decomposition corresponds to real measurement and can be fitted in the frame of the IM in this case. New statistical parameters describing the properties of experimental equipment (irrespective to their internal "filling") are found. The suggested approach is rather general and can be used for calibration and comparison of different complex dynamical systems in practical purposes.*

*Keywords: complex systems, X-ray diffractometer, corundum, Fourier and Prony's decompositions, data treatment analysis, ideal experiment, intermediate model.*

It is becoming evident that the fundamental and simple (from the mathematical point of view) rules that have been established earlier for simple systems are difficult to find and then (if they were found) to justify for different complex systems. In order to understand better the behavior of a complex system that does not have the "best fit" model (containing a relatively small number of fitting parameters), based on simple physical principles, it is necessary to find some *general principles* that might exist in a wide class of phenomena. General principles are hidden and covered by uncontrollable factors known in measurements as an influence of random fluctuations or "noise". In order to decrease the effects of these high-frequency fluctuations many experimentalists repeat their measurements many times having in mind the conventional statistical paradigm: the repetition of $N$ measurements of the *uncorrelated* random sequence should decrease the amplitude of noise by a factor of $1/N^{1/2}$. But the hypothesis that noise is really uncorrelated is, in many cases, an unjustified *supposition*. So, the key question to be formulated: are there some justified (or verified) arguments that might test this supposition and take into account the influence of the measured equipment? In many cases the successive measurements have strong correlations and so the conventional paradigm ($1/N^{1/2}$) does *not* work and should be replaced by more general and verified scheme.

In papers [1-3] based on different experiments it was proved that many successive measurements are strongly-correlated and actually *remember* each other. The solutions of the corresponding functional equations that mathematically reflect the fact of a *memory* presence lead us to reconsidering the conventional supposition and to formulate a new concept of measurements that is based on an *intermediate* model (IM). This IM has a set of parameters that is small in comparison with number of initial data points and provides a good fit of the measured curve when the "best fit"/specific model based on some physical principles is *absent*. We define the governing principle by an evolution of the repeated measurement process as the Quasi-Periodic (QP) process and describe its general properties. The further continuation these ideas were received in papers [4-6] where it has been proved that for *all* reproducible measurements can be expressed in terms of the IM. This statement was proved on some available and reproducible data. Besides, in the frame of new approach it becomes possible to eliminate the

* *email: renigmat@gmail.com*

influence of the apparatus function (AF) and reduce all measurements to an *ideal* experiment. After elimination of the random factors accompanying each process of measurements one can prove that the IM for ideal experiment is reduced to the fitting of the measured function by the fragment of the Fourier series.

This paper serves as a logical continuation of the previous papers [1-6] and can be used in observation of the dynamics of different complex systems. We want to demonstrate another important application of the suggested conception. Practically, one can use two XRDs taken from two different producers (one was labelled as A-XRD ("cheap") and another one B-XRD ("expensive")) and compare their spectral characteristics in the frame of the unified intermediate model IM). The new QP-concept allows fitting the measured data in the frame of parameters that describe the AFR (amplitude-frequency response) reflecting the decomposition to the generalized Prony's spectrum (GPS). Therefore, the problem that is considered in this paper can be formulated as follows:

- to show and justify some criteria that helps detecting the presence of QP process in the repeated experimental measurements;

-to show a proper solution of the corresponding functional equation, while this solution yields the description of the identified QP process;

- to suggest some computing algorithm for fitting of the actual data to the analytical function that follows from the solution of the corresponding functional equation.

The content of this paper is organized as follows. In the section 2 we give some important details of describe the measured X-ray spectra. This information can be useful for comparison of other possible equipment. In section 3 we remind briefly the basic principles outlined previously in papers [1-6] and add some new and significant elements that can be important for creating a suitable algorithm. Section 4 summarizes the results and outlines the perspectives of this approach for the quantitative description of time-dependent reproducible data that are registered in different systems and devices. Here we should note that under the *complex system* we imply a system where a conventional model is *absent* [7]. Under *simplicity* of the acceptable model we imply the proper hypothesis ("best fit" model) containing a minimal number of fitting parameters that describes the behaviour of the system *quantitatively*. The different approaches that exist nowadays for the description of different complex systems are collected in the recent review [8].

## Experimental part

The measurements are performed in two diffractometers with main characteristics that are listed below.

*A – XRD.* The characteristics of the XRT: power – 10 Wt., working voltage – 25 kV, the working current 0.4 mA. The anode is made from iron, the primary radiation – Fe $K_\alpha$, the wavelength consists 1.93728A°. The used detector is positionally-sensitive gas detector (PSGD) with 4096 channels. The working range of angle measurements $2\theta \approx 17\text{-}76^\circ$ and each certain diffraction angle is fixed in each channel. The asymmetric scheme of recording is explained schematically by figure 1(a). A set of diffractograms was obtained in the range of angles $2\Theta = 19.32\text{-}73.9^\circ$ with the fixed step 0.02°. From the total diffractogram spectrum the range of angles $2\theta = 25.96 - 37.16^\circ$ was extracted. A typical spectral curve recorded for the first corundum reflex is given in figure 1(b).

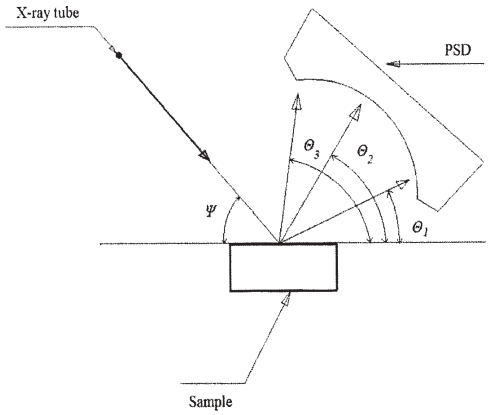


Fig.1(a). The typical measurement scheme realized for A ("cheap") - XRD. ψ is a constant angle of incidence. The angle of reflection accepts different values $-\Theta_i$. The acronym PSD signifies the positionally sensitive detector.

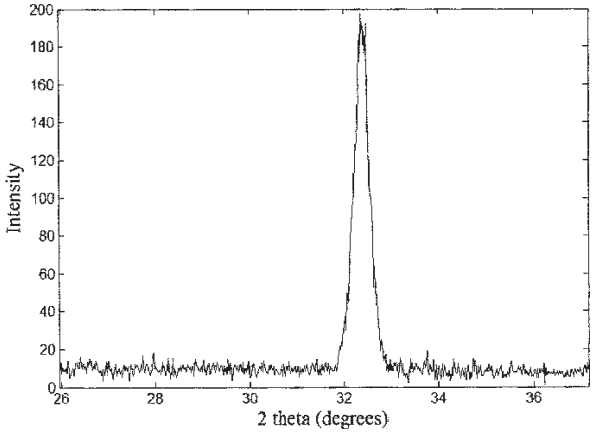


Fig.1(b). Typical diffractogram recorded from the corundum first reflex and obtained with the help of the A - XRD

*B – XRD.* X-ray tube (XRT): Power – 1600 Wt., working voltage – 40 kV, working current – 40 mA. The material of anode made from copper, primary radiation – Cu $K_\alpha$, with the fixed wavelength – 1.5418A°. It has semiconducting detector with 192 channels. The registration of the secondary radiation was performed in one-channel regime and one channel contains 9 strips. Before XRT and detector the slits were established with clearance 0.6 mm. Besides, for decreasing of the divergence of the initial X-ray beam two Soller slits (vertical with 2.5 degrees for the primary radiation and horizontal slit having the same angle for reflected radiation) were used. The total number of points is remained the same (equaled 560) as for diffractograms obtained for the A-XRD described above. Exposition time of each diffractogram occupied 900 s with interval between measurements 30 s. The symmetric (Θ-Θ) scheme for diffractograms recording is depicted schematically on figure 2(a). The set of diffractograms was obtained in the range of angles $2\Theta = 24.8\text{-}26.2^\circ$ with the fixed step 0.0025°, exposition time for one point equaled 1 s. Each diffractogram contains 560 data points and temporal interval between successive measurements occupies 39 s. Typical diffractogram is depicted on figure 2(b). The statistical characteristics are given in table 1 with the same notations. The total time for obtaining of 20 measurements occupied 199.5 min. The statistical characteristics for all 20 diffractograms are listed in table 1, where $N_{tot}$ defines the total number of digit pulses collected for one spectral curve, $N_{max}$ defines the maximal number of digit pulses collected for one data point, the <CPS> defines the mean velocity of digit pulses per second.

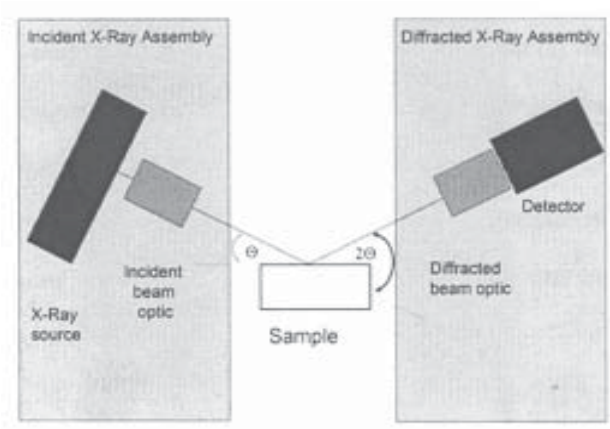


Fig.2(a). The symmetrical scheme for recording of diffractograms realized on the B ("expensive") - XRD. The incident angle Θ is fixed and X-ray source together with detector change their positions simultaneously in order to pass through the whole sample

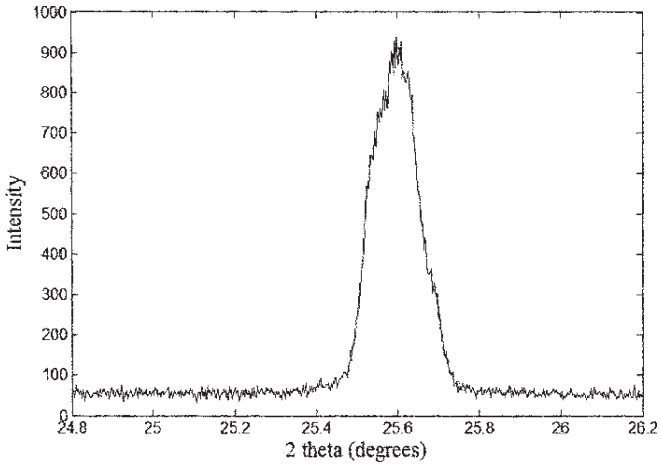


Fig.2(b). Typical diffractogram recorded from the corundum first reflex and obtained with the help of the B - XRD.

| Number of measurement | B (expensive")- XRD | | | A ("cheap")- XRD | | |
|---|---|---|---|---|---|---|
| | $N_{tot}$ | $N_{max}$ | <CPS> | $N_{tot}$ | $N_{max}$ | <CPS> |
| 1 | 80436 | 937 | 143 | 8928 | 197 | 50 |
| 2 | 80835 | 999 | 144 | 8847 | 191 | 50 |
| 3 | 80810 | 957 | 144 | 8872 | 205 | 50 |
| 4 | 80553 | 937 | 143 | 8768 | 191 | 49 |
| 5 | 80615 | 913 | 144 | 8837 | 193 | 49 |
| 6 | 81105 | 950 | 145 | 8856 | 203 | 50 |
| 7 | 80630 | 964 | 144 | 8821 | 200 | 50 |
| 8 | 80416 | 911 | 143 | 8916 | 185 | 50 |
| 9 | 80326 | 946 | 143 | 8916 | 193 | 50 |
| 10 | 80535 | 938 | 143 | 8935 | 198 | 50 |
| 11 | 80265 | 928 | 143 | 8945 | 200 | 49 |
| 12 | 80246 | 930 | 143 | 8873 | 194 | 49 |
| 13 | 81293 | 950 | 145 | 8829 | 188 | 49 |
| 14 | 80949 | 926 | 144 | 8788 | 203 | 49 |
| 15 | 80818 | 995 | 144 | 8651 | 185 | 49 |
| 16 | 79941 | 942 | 142 | 8721 | 196 | 49 |
| 17 | 80282 | 924 | 143 | 8858 | 210 | 49 |
| 18 | 80532 | 915 | 143 | 8840 | 210 | 49 |
| 19 | 80712 | 972 | 144 | 8946 | 203 | 49 |
| 20 | 80425 | 929 | 143 | 8801 | 202 | 49 |

**Table 1**
THE COMPARATIVE CHARACTERISTICS OF TWO DIFFRACTOGRAMS OBTAINED FOR CORUNDUM ($\alpha$-$Al_2O_3$). THE PARAMETERS ARE EXPLAINED IN SECTION 2

In these experiments we measured the *same* substance. As the measured object we chose corundum ($\alpha$-$Al_2O_3$). The selection of this object was dictated by the following reasons: it has narrow diffraction peaks and it is used frequently for calibration and adjustment purposes. The corundum structure is well-known: it represents a crystal structure with symmetry described by the space group $R^3c$ with constants of the lattice $a$=4.7540A° and $c$=12.9900 A° (hexagonal arrangement). We did not put a problem of determination of a structure of this substance. So, we measured only the first reflex from the planes with index (102) and interplanar spacing $d$=3.477 A°.

*Description of the treatment procedure*

The QP-processes and the basic functional equations

In the beginning of this section we want to remind the basic principles (taken from papers [1-6]) that can lead to existence of the QP-processes in real measurements. It is well-known that a pure periodic process with a given period $T$ satisfies to the following functional equation

$$\Pr(t+T) = \Pr(t). \quad (1)$$

From the experimental point of view, relationship (1) corresponds to an "ideal" experiment where all successive experiments remained the *same* and coincided with the first one. The general solution of this functional equation is known and it can be expressed in the form of the Fourier series decomposition (usually the measured function is defined on the discrete set of the given points $[t_j]$ $j$=1,2,...,$N$).

$$\Pr(t) = A_0 + \sum_{k=1}^{\infty}\left[ Ac_k \cos\left(2\pi k \frac{t}{T}\right) + As_k \sin\left(2\pi k \frac{t}{T}\right)\right]. \quad (2)$$

So, from the concept of *ideal* experiment the Fourier decomposition accepts new interpretation and corresponds to the *absence* of a memory (in other words, the absence of correlations between successive measurements). Instead of equation (1) we consider more general functional equation

$$F(t+T) = aF(t) + b, \qquad (3)$$

where the parameters $a$ and $b$ represent real constants. This functional equation means that: temporal evolution of some process taking place on the interval $t > T$ is based on events (measurements in our case) that took place presumably in the nearer past ($t < T$). This functional equation was considered for the first time in [9] but in the present paper we want to generalize it. The solution of this equation can be written in the following form [9]

$$a \neq 1:\ F(t) = \exp\left(\lambda \frac{t}{T}\right)\mathrm{Pr}(t) + c_0,\ \ \lambda = \ln(a),\ c_0 = \frac{b}{1-a},$$
$$a = 1:\ F(t) = \mathrm{Pr}(t) + b\frac{t}{T}. \qquad (4)$$

If $a > 1$ then we have the *increasing* exponential factor ($\lambda > 0$). The period $T$ is supposed to accept only *positive* values. For this situation the influence of the past events on the present event is becoming *essential*. For $a < 1$ we have the effect of the exponential decay ($\lambda < 0$) and, in this case, the influence of the past events (that were take place for $t < T$) upon the present event ($t > T$) is not essential. For $a = 1$ ($b \neq 0$) we have alongside with periodic oscillations the appearance of a linear temporal trend and, finally, for $a = 1$ and $b = 0$ the solution (4) is reduced to the conventional Fourier solution (2). If we associate the function $F(t)$ with some measurement then the functional equation (3) can be interpreted as follows. The second measurement (realized after period $T$ and associated with the duration of one experiment) being plotted with respect to the previous measurement forms a curve close to a segment of straight line. It means that the second measurement is strongly-correlated with the previous one. It is easy to prove (by mathematical induction) that other successive measurements performed in later periods, also satisfy to the functional equation (3) but in this case the parameters $a$ and $b$ depend on a number of successive measurement

$$F(t+sT) = a_s F(t) + b_s, \qquad (5)$$

The constants $a_s$ and $b_s$ ($s = 1,2,\ldots,M$) where $M$ defines here and below the last measurement can be found with the help of the recurrence relationships

$$a_{s+1} = a_1 a_s,\ \ b_{s+1} = a_s b_1 + b_s,$$
$$s = 1,2,\ldots M, \qquad (6)$$

or numerically, with the help of the linear least square method (LLSM).

Equation (3) admits the following generalization [2-3]

.

$$F(t+LT) = \sum_{s=0}^{L-1} a_s F(t+sT) + b. \qquad (7)$$

This functional equation describes mathematically a wide class of the QP processes and can be interpreted as follows. The measurement process that takes place during the interval $[(L\text{-}1)T, LT]$ partly depends on the processes that have been happened in the previous temporal intervals $[sT, (s+1)T]$ with $s$=0,1,..., $L$-2. The set of the constants $\{a_s\}$ ($s$ = 0,1,...,$L$-1) can be quantitatively interpreted as the influence of a memory between successive measurements. In comparison with the functional equation (7), expression (3) can be interpreted as a system having the *shortest* memory. The solution of the generalized functional equation (7) can be presented in two forms

$$\sum_{s=0}^{L-1} a_s \neq 1:\ F(t) = \sum_{r=1}^{L} \exp\left(\ln(\kappa_r)\frac{t}{T}\right)\mathrm{Pr}_r(t) + c_0,\ \ c_0 = \frac{b}{1-\sum_{s=0}^{L-1} a_s}, \qquad (8a)$$

$$\sum_{s=0}^{L-1} a_s = 1:\ F(t) = \sum_{r=1}^{L} \exp\left(\ln(\kappa_r)\frac{t}{T}\right)\mathrm{Pr}_r(t) + c_1\frac{t}{T},\ \ c_1 = \frac{b}{L-\sum_{s=0}^{L-1} s\cdot a_s}. \qquad (8b)$$

Here the functions $\mathrm{Pr}_r(t)$ define a set of periodic functions from expression (2) and $\kappa_r$ ($r$=1,2,...,$L$) coincide with the roots of the characteristic polynomial

$$P(\kappa) = \kappa^L - \sum_{s=0}^{L-1} a_s \kappa^s = 0. \qquad (9)$$

In general, these roots can be positive, negative, $g$-fold degenerated (with degeneracy value $g$) and complex-conjugated. We should note also that for the case (8b) one of the roots $\kappa_r$ coincides with the unit value ($\kappa_1 = 1$) that leads to the pure periodic solution. As before, the finite set of the unknown periodic functions $\mathrm{Pr}_r^{(T)}(t)$ ($r$= 1,2,...,$L$) is determined by their decomposition coefficients $Ac_k^{(r)}, As_k^{(r)},\ r = 1,2,\ldots,L;\ k = 1,2,\ldots,K$.

$$\mathrm{Pr}_r^{(T)}(t) = A_0^{(r)} + \sum_{k=1}^{K>>1}\left[Ac_k^{(r)}\cos\left(2\pi k\frac{t}{T}\right) + As_k^{(r)}\sin\left(2\pi k\frac{t}{T}\right)\right] \qquad (10)$$

We want to emphasize here the following fact. The conventional Prony decomposition [10-12] does not have any specific meaning and was considered as an alternative decomposition alongside with other transformations (Fourier, wavelet, Laplace and etc.) used in the signal processing area. Nevertheless, in paper [1] we found an *additional* meaning of this decomposition and now it can imply that exponential multipliers figuring before periodic functions can have *not* only real, but also decaying values. Solution (8) has general characteristics and other roots from algebraic equation (9) can modify essentially the conventional solution. All possible solutions of the general functional equation (7), for different types of roots, are considered in papers [1-3, 7-9].

Decompositions (8)-(10) have a clear meaning and correspond to the *linear* presentation of a possible memory that can exist between repeated measurements. These coefficients reflect also the influence of uncontrollable factors from the measuring equipment used and this important factor is *not* taken into account in the conventional data processing. The memory effect (considered for the discrete set of data) is expressed quantitatively by the enumerable set of real constants $\{a_s\}$ figuring in equation (7). In this sense the process without memory (the so-called Markovian process) corresponds to the following set of constants: $a_0 = 0$, $a_1 = 0$, ... , $a_{L-1} = 1$ and its solution coincides with a pure periodic function (2). This solution corresponds to an *ideal* experiment, as it has been mentioned above. In this sense the IM coincides with presentation of the measured data by means of the Fourier spectrum. From another side, the conventional expression for the mean function when in expression (7) $\langle F(t)\rangle \cong F(t+(N+1)T)$ and $a_s = 1/N,\ b = 0$ can be inter-

preted as the process having a *uniform* memory. This process coincides with the conventional *supposition*, but in practical terms cannot be performed, because it is very difficult to follow the condition $a_s = 1/N$, $b = 0$, corresponding to the case of the uniform memory. As it will be shown below, the relationship (3) is realized for the given data with high accuracy (with relative error < 10%, see expression (12) below) and, so, the measured data can be approximated with the help of the fitting function (4), which can be presented in the following and convenient (for numerical calculations) form

$$F(x;K,T) = B + E_0 \exp\left(\lambda\frac{x}{T}\right) + \sum_{k=1}^{K}\left[Ac_k yc_k(x) + As_k ys_k(x)\right],$$
$$yc_k(x) = \exp\left(\lambda\frac{x}{T}\right)\cos\left(2\pi k\frac{x}{T}\right),\ ys_k(x) = \exp\left(\lambda\frac{x}{T}\right)\sin\left(2\pi k\frac{x}{T}\right). \quad (11)$$

We should stress here the following fact. Usually, the variable $x$ in many experiments cannot coincide with the current time $t$. For example, instead of temporal variable $t$ in spectral measurements the scattering angle ($\theta$), the inverse wavenumber ($\lambda^{-1}$) and number of data points ($x_j = j$; $j = 1,2,\ldots,N$) can be used also. For these types of experiments the true value of the period $T(x)$ is *unknown* and calculation of this important parameter represents a *separate* problem. Below we want to show *how* to solve this problem in our case and then calculate the optimal value of nonlinear parameter $T_{opt}$ associated with number of the measured points. If one can decompose the measured data by means of the fitting function (11), then it can be used as the *intermediate* model. It contains $2K+4$ fitting parameters [$\lambda$, $B$, $E_0$, $Ac_k$, $As_k$ ($k = 1,2,\ldots K$) and $T(x)$] that form the desired AFR, corresponding to the Prony's decomposition (11). This decomposition is *not* arbitrary. It follows from natural condition (5) that can be tested and justified for any partial experiment. In fact, the total set of parameters should satisfy to the condition: $2K+4 << N$ and only in this sense the IM can be considered as an actual/effective replacement of random functions figuring in repeated measurements. We should pay attention to the damping constant $\lambda(a) = \ln(a)$ figuring in (4) because it is *not* an independent parameter. It reflects the influence of the device (defined as a set of uncontrollable external factors) and depends totally on the value $a$ that, in turn, is calculated *numerically*. In order to find the optimal value of the $T_{opt}$ we notice that this value should be located in the interval [$0.5\,T_{max}$, $2T_{max}$], where the value of $T_{max}(x)$, in turn, should be defined as $T_{max}(x) = \Delta x \times L(x)$ ($\Delta x$ is a step of discretization and $L(x) = x_{max} - x_{min}$ is a length of the interval associated with the current variable $x$). This important observation helps to find the optimal values of $T_{opt}$ and $K$ from the procedure of minimization of the relative error that exits between the measured function $y(x)$ and the fitting function (11). We use the conventional definition of this expression for relative error that minimizes the quadratic deviations

$$\min(\mathrm{Re}lErr) = \left[\frac{stdev\left(y(x) - F(x;T_{opt},K)\right)}{mean|y|}\right]\cdot 100\%,$$
$$1\% < \min(\mathrm{Re}lErr(K)) < 10\%,\ T_{opt} \in [0.5T_{\max}, 2T_{\max}], \quad (12)$$
$$T_{\max} = \left(x_j - x_{j-1}\right)\cdot L(x).$$

The calculations show that instead of minimizing of the surface RelErr($T$,$K$) with respect to the two unknown variables $T$ and $K$, we can minimize the cross-section at the fixed value of $K$. This initially chosen value of $K$ should satisfy to the condition that is given by the second row of expression (12). If the supposition is correct, then all measured data can be fitted in the frame of the intermediate hypothesis (11) and compared in terms of their AFRs. Schematically this new presentation of data can be expressed as

$$y(x) \cong F(x) \Rightarrow AFR(\lambda, T_{opt}, B, E_0; Ac_k, As_k)$$
$$k = 1,2,\ldots,K,\ x \equiv x_j,\ j = 1,2,\ldots N. \quad (13)$$

Namely, these fitting parameters form the desired decomposition in the Prony's spectrum and define the desired AFR.

*The proposed algorithm*

As it was mentioned in section 2 we obtained 20 successive measurements ($s$ = 1, 2, … , $M$=20) for each calibrated device labelled above as (B-) and A-XRD. If we combine their spectra together with respect to the *same* number of the measured points (i.e., 560) then we obtain the picture depicted on figure 3(a).

*Step 1* - Normalization procedure.

In order to compare spectral curves measured for two different types of XRD in terms of the fitting parameters (13) we can normalize all measures:

$$Nrm_s(x) = \frac{y_s(x)}{MV},\ MV = \frac{1}{M}\sum_{s=1}^{M}\max(y_s(x)). \quad (14)$$

Here $\max(y_s(x))$ defines the maximal value of each successive measurement. These normalized spectra are shown on figure 3(b). In order to see the initial differences between the spectra belonging to different spectrometers one can calculate the following values

$$mn_s = \frac{mean(y_s(x)}{MnV},\ MnV = \frac{1}{M}\sum_{s=1}^{M} mean\left(y_s(x)\right),$$
$$mx_s = \frac{\max(y_s(x)}{MV},\ MV = \frac{1}{M}\sum_{s=1}^{M}\max\left(y_s(x)\right). \quad (15)$$

They are depicted onfigure 3(c). As one notice from this figure the values corresponding to the A- XRD are more deviated in comparison with the values corresponding to the B-type.

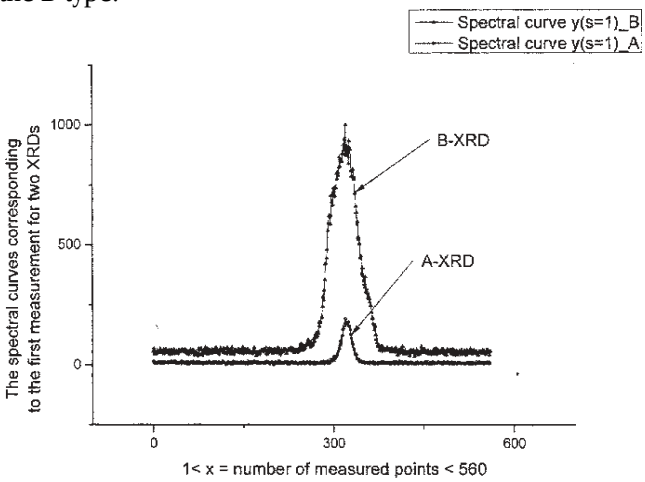


Fig.3(a). Here we demonstrate two combined spectral curves corresponding to the first measurement ($s$=1) for two types of devices labelled as B- and A - XRDs. In order to compare them with each other we should normalize their intensities in accordance with expression (14)

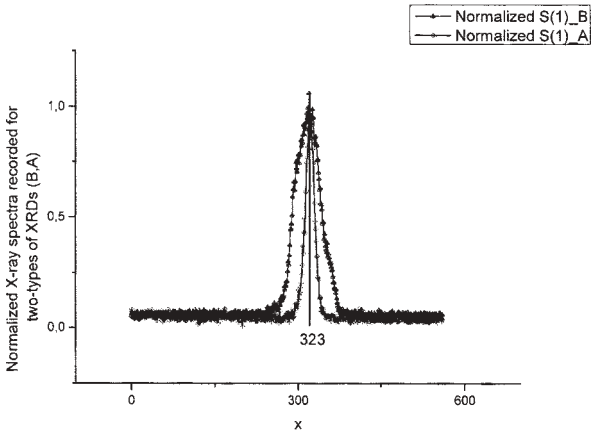


Fig.3(b). Here we show the normalized spectral curves (the first measurement $y(s=1)$ for both XRDs) that are used for comparison of their statistical characteristics. Number of the measured points (equaled 323) shows the position of extreme point.

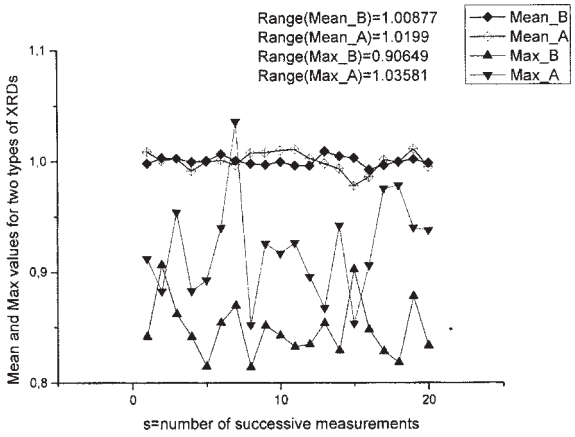


Fig.3(c). The distribution of the normalized mean and maximal values for the 20 measurements. This preliminary statistical information can be used for initial comparison of two diffractometers. As one can notice from this figure the deviations for the A-type XRD visually look larger.

*Step 2* - The derivation of the functional equation for average values.

If we consider two successive measurements, then as it follows from equation (3) we can write

$$\begin{aligned} &F(t+sT)=aF(t+(s-1)T)+b, \\ &s=1,2,...,M-1. \end{aligned}, \qquad (16)$$

This means that if the supposition (3) is correct, then $a$ and $b$ in (16) should keep their constant values for all measurements. However, in real measurements these values change due to the influence of different *uncontrollable* factors that are appeared in each measurement. In fact, these variations should reflect the quality of the whole measurement procedure. In this line of thought, relationship (16) is replaced for more realistic equation

$$\begin{aligned} &F(t+sT_s)=a_sF(t+(s-1)T_s)+b_s, \\ &s=1,2,...,M-1. \end{aligned}, \qquad (17)$$

where the constants $a_s$ and $b_s$ and the nonlinear parameter $T_s$ can be found numerically from equation (12). So, after making these preliminary calculations we should check the relationship (17) and find the variations of the constants $a_s$ and $b_s$. The approximate correspondence to the segment of a straight line is shown in figures 4(a,b), where the strong correlation between the first measurement $y(s=1)$ to the second one $y(s=2)$ for two types of XRD is shown. Again, one can notice that standard deviations for the first B-XRD is smaller (fig.4(a)) than the same segments depicted for the A-XRD in figure 4(b). The calculated values of $a_s$ (coinciding with a set of slopes) and $b_s$ (defining the set of intercepts) are given by figures 4(c,d), correspondingly. Figure 4(e) demonstrates the distribution of the values of $\lambda_s$ for two types of XRDs. The optimal values of $T_s$ should be calculated from expression (12). For example, figure 5 shows the dependence of the relative errors with respect to the values of the period taken from the admissible interval $[0.5\,T_{max}, 2T_{max}]$ for the first spectral curve $y_1(s=1)$ corresponding to the two types of XRDs. Now we can put forward an interesting question: what kind of statistically significant parameters can characterize the "quality" of each XRD? Definitely, the internal structure of the given diffractometer is considered in both cases as a "black box". From our point of view, the answer is contained in relationship (17). We know that "ideal" (perfect) experiment should give for all measurements $a=1$ and $b=0$. If we take the mean values from the calculated constants of $a_s$ and $b_s$

$$\langle a\rangle=\frac{1}{M}\sum_{s=1}^{M}a_s,\ \langle b\rangle=\frac{1}{M}\sum_{s=1}^{M}b_s, \qquad (18)$$

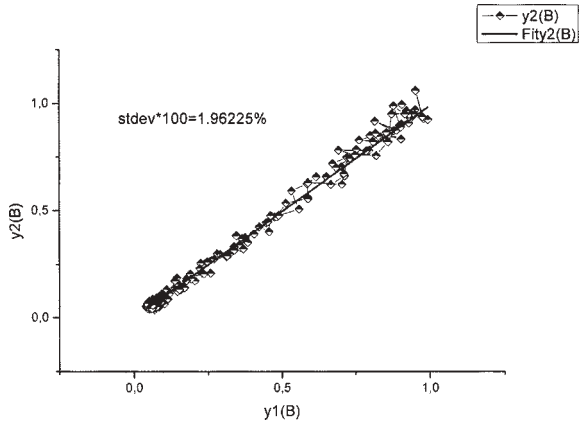


Fig.4(a). Two successive measurements $y(s=1)$ and $y(s=2)$ being plotted with respect to each other form a curve close to a segment of the straight line. The value of standard deviation in the center of the figure shows the deviation of the second measurement with respect to the first one.

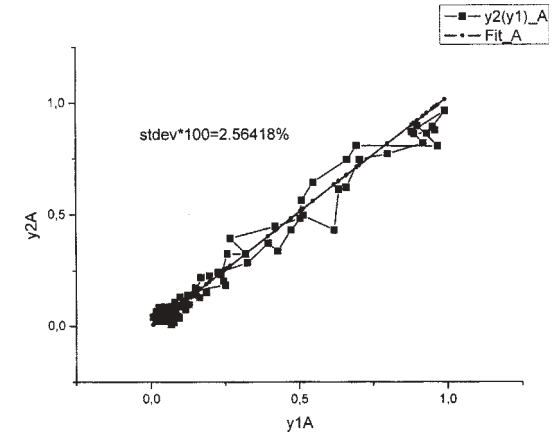


Fig.4(b). The same dependence for two spectral curves $y(s=1)$ and $y(s=2)$ is observed for the A-XRD but standard deviations in comparison with B-diffractometer shown on figure 4(a) are becoming larger

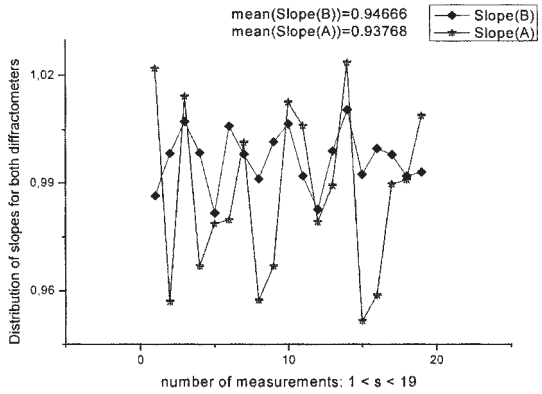


Fig.4(c). The distributions of the slopes for two types of diffractometers are shown. As one can notice from this figure the deviations from mean value corresponding to B-XRD (black rhombs) are smaller in comparison with A - diffractometer (marked by stars).

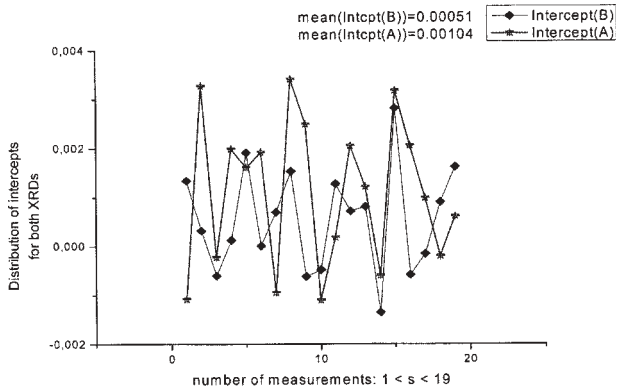


Fig.4(d). The distributions of the intercepts for two types of diffractometers are shown. As before, the deviations of intercepts (black rhombs) from its mean value corresponding to B-XRD are smaller in comparison with A - diffractometer (marked by stars). So, one can conclude that B-XRD is closer to an "ideal" device.

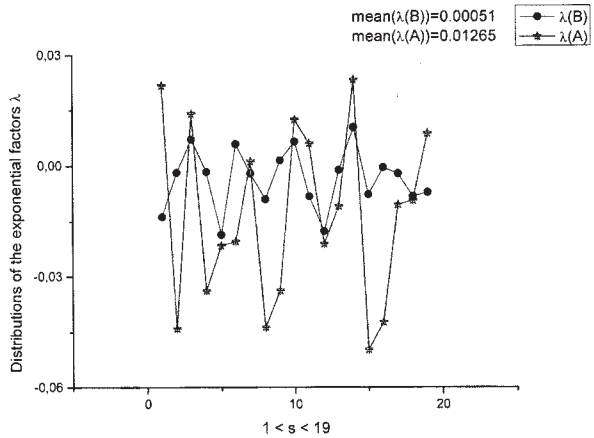


Fig.4(e). The distribution of the exponential damping factors λ for two types of diffractometers. Again the B-XRD justifies its definition as "expensive" one because its deviations are concentrated closer in the vicinity of its mean value.

then we obtain the objective *quantitative measure* that allows us to compare the "perfection" of each diffractometer used and its deviation from an "ideal" device ($a$ = 1, $b$ = 0). As it follows from figures 2(c,d) the mean values of the slopes and intercepts calculated for two XRDs (B, A) are the following: $<a>$ = 0.9467(B), 0.9377(A); $<b>$ =0.00051(B), 0.00104 (A). From analysis of these values the obvious conclusion follows: the B-XRD is closer to an "ideal" device in comparison with the "A"-type. The new approach justifies the functional equation (3) and its

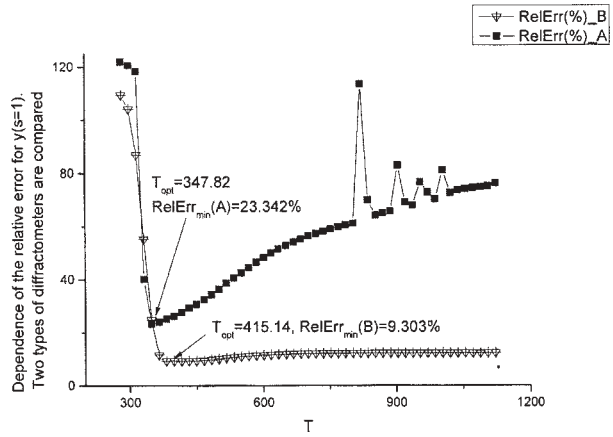


Fig.5. This figure explains the procedure of the finding the value of $T_{opt}$ from expression (12). The existence of the corresponding minimal value of the relative error located in the interval [0.5 $T_{max}$, 2$T_{max}$] should coincide with this value. As an example two spectral curves $y(s=1)$ for two XRDs were chosen.

more general form (17) allows us to realize the Prony's decomposition of each measurement *separately* or, to provide the final fit in accordance with equation

$$\langle F(t+<T>)\rangle = <a>\langle F(t)\rangle + <b>,$$
$$\langle F(t)\rangle = \frac{1}{M}\sum_{s=1}^{M} F_s(t). \qquad (19)$$

*3. Step* - Calculation of the desired AFR for successive and mean spectral curves**.**

Finally one can fit the measured set of curves (16) or mean function (19) to the function (11) in order to calculate the desired set of fitting parameters that form the AFR. In order not to overload the content of the paper by a high number of figures we show only the fit of mean spectral curves (19) and their AFR for comparing the two types of XRDs. Figures 6(a,b) show the final (perfect) fit of the mean spectral curves for two types of diffractometers by fitting function (11), figures 7(a,b) represent their AFRs, where it was used the same number of decomposition coefficients (modes) ($K$=15) providing the values of the relative error 4.01% and 10.05% for B-, A-diffractometers, accordingly. Other parameters that are important for comparison of these two devices are collected in tables 2 and 3. So, for completeness of this analysis we can find 34 fitting parameters that are sufficient for the fitting of the mean spectral curves characterizing the two types of the spectrometers in the frame of the IM concept. Here we want to stress the following: in spite of the measurement

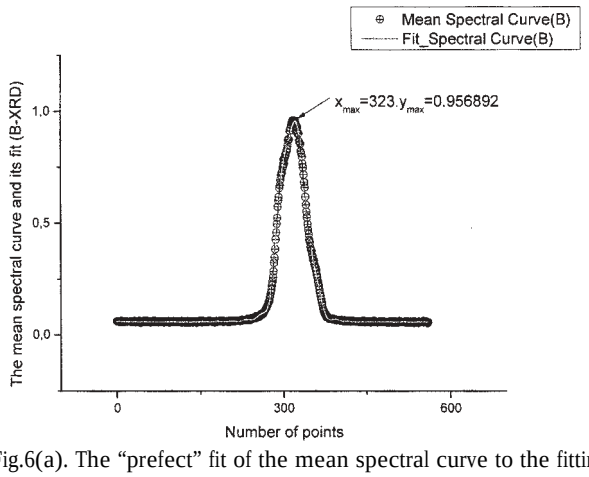


Fig.6(a). The "prefect" fit of the mean spectral curve to the fitting function (11) corresponding to the B-XRD is shown. All additional fitting parameters including the value of the fitting error are shown in table 3

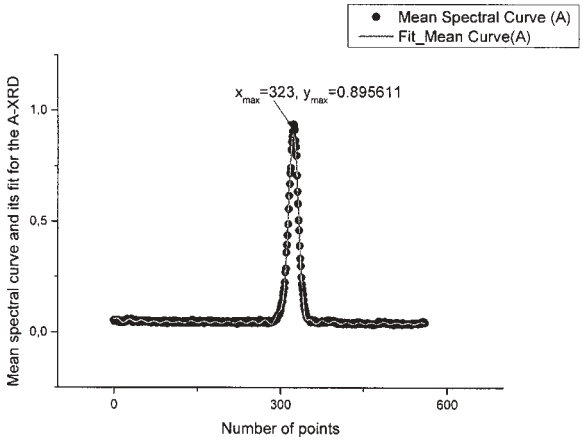


Fig.6(b). The "prefect" fit of the mean spectral curve to the fitting function (11) corresponding to the A-XRD is shown. All additional fitting parameters including the value of the fitting error are shown in table 3

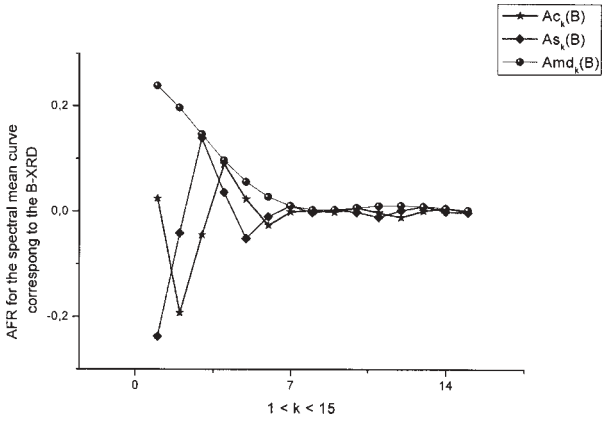


Fig.7(a). The AFR that corresponds to the fit of the mean curve for the B-XRD. The balls show the behavior of the parameter $Amd_k = \sqrt{Ac_k^2 + As_k^2}$ All numeric values of these plots are collected in table 2

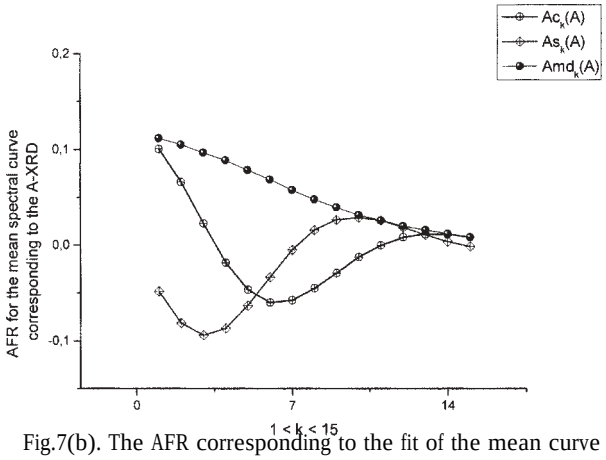


Fig.7(b). The AFR corresponding to the fit of the mean curve for the A-XRD. The balls, as before, show the behaviour of the function $Amd_k = \sqrt{Ac_k^2 + As_k^2}$ . It is interesting to note the AFR for the A-XRD has smooth behavior while for the coefficients $Ac_k$ and $As_k$ depicted in figure 7(a) this monotone dependence is absent. All numeric values describing this dependence are collected in table 2

| Number of mode $k$ | B- XRD | | | A- XRD | | |
|---|---|---|---|---|---|---|
| | $Ac_k$ | $As_k$ | $Amd_k$ | $Ac_k$ | $As_k$ | $Amd_k$ |
| 1 | 0,0246 | -0,23732 | 0,23859 | 0,10055 | -0,04837 | 0,11158 |
| 2 | -0,1925 | -0,04131 | 0,19688 | 0,0661 | -0,08127 | 0,10476 |
| 3 | -0,04486 | 0,13954 | 0,14658 | 0,02269 | -0,09394 | 0,09664 |
| 4 | 0,08998 | 0,03675 | 0,09719 | -0,01864 | -0,0868 | 0,08878 |
| 5 | 0,02324 | -0,05169 | 0,05668 | -0,04678 | -0,06305 | 0,0785 |
| 6 | -0,02614 | -0,0097 | 0,02789 | -0,05996 | -0,0336 | 0,06873 |
| 7 | -8,6442E-4 | 0,01079 | 0,01082 | -0,05731 | -0,0053 | 0,05756 |
| 8 | 0,00249 | -0,0024 | 0,00346 | -0,04528 | 0,01557 | 0,04788 |
| 9 | -0,0012 | 0,00327 | 0,00348 | -0,02939 | 0,02637 | 0,03949 |
| 10 | 0,00741 | -0,0013 | 0,00753 | -0,01283 | 0,02877 | 0,0315 |
| 11 | -0,00249 | -0,01044 | 0,01073 | -6,17303E-4 | 0,02571 | 0,02572 |
| 12 | -0,01122 | 0,00217 | 0,01143 | 0,00781 | 0,01817 | 0,01978 |
| 13 | 0,00117 | 0,00938 | 0,00945 | 0,01141 | 0,01055 | 0,01554 |
| 14 | 0,00596 | -2,25382E-4 | 0,00597 | 0,0111 | 0,00329 | 0,01158 |
| 15 | -3,65397E-4 | -0,00227 | 0,0023 | 0,00795 | -0,00168 | 0,00813 |

**Table 2**
WE DECIDED TO GIVE *ALL* FITTING PARAMETERS THAT FORM THE DESIRED AFRs BECAUSE OF THEIR IMPORTANCE. THE CORRESPONDING PLOTS ARE PRESENTED BY FIGURES 7(a,b)

| Type of XRD | $T_{opt}$ | λ | $E_0$ | $B$ | Range(Amd) | RelErr(%) |
|---|---|---|---|---|---|---|
| B ("expensive") | 415,14 | -0,00337 | 0,40135 | -0,21501 | 0,23629 | 3,96674 |
| A ("cheap") | 347,82 | -0,01265 | 0,46606 | -0,36104 | 0,10345 | 10,0537 |

**Table 3**
ADDITIONAL FITTING PARAMETERS CHARACTERIZING THE FIT OF MEAN CURVES DEPICTED ON FIGURES 6 (a,b)

The definition Range(Amd) in column 6 signifies the value: Range(Amd) = max(Amd) – min(Amd), $Amd_k = \sqrt{Ac_k^2 + As_k^2}$

of the *same* substance their AFRs are statistically *different*. We explain this difference by the influence of X-ray beam having different intensities and wavelengths for each diffractometer used. Besides this general explanation we associate this difference with different constructive peculiarities of the XR detector. In construction of the B-XRD the stable and sensitive semiconducting detector is applied while in another device A-XRD the PSGD having lower sensitivity and stability in detection of the reflected X-ray beam was used.

## Results and discussions

In this section we want to list the basic results that were received in this paper.

The Fourier-transform receives an *extended* interpretation and can be used as an IM for description of "ideal" experiment without memory.

The Prony's decomposition should be used as an IM for quantitative description of a set of successive measurements with memory.

Intermediate model contains a set of quantitative parameters that can characterize experimental equipment from *statistical* point of view *irrespective* to its internal "filling". The measured device in this sense can be considered as a "black" box.

Successive measurements can create a sampling that can characterize a "proximity" to an "ideal" experiment.

Normalization procedure expressed by relationships (14) and (15) becomes useful in cases when the measured data obtained from different devices are strongly deviated from each other. It helps to decrease the essential differences between two types of data and makes close the statistical characteristics of two devices compared.

## Conclusions

Discussing these results we can add the following:

- we suppose that the Prony's decomposition allows fitting many types of different and initially random data with trend in terms of the justified IM. This assertion needs in further confirmations;

- in modern science the wide usage of the Fourier-transform is based presumably on the clear "physics" of this transformation. Now the *competitive* Prony's decomposition and its AFR also are needed in clear interpretation because they can describe the "physics" of many real experiments;

- IM in many cases (when the simple and "best fit" model is *absent*) can solve the problem of reduction of data, when initial data $N$ points are reduced to $(2K+2)L+1 << N$ ($L$ defines a set of roots from (9)) a relatively short number of parameters describing the AFR of the found Prony's spectrum. In opens new possibilities in comparison of many complex spectra (obtained from different spectral equipments, at least) in terms of their AFRs that are calculated from the *same* IM;

- in the frame on new approach it becomes possible to introduce the unified calibrations curves that can be expressed in the form of straight lines (conventional presentation) or in the form of nonlinear curves that can be common for different equipments. The conception of the IM together with its quantitative label (AFR) can play a decisive role in constructive of new types of calibration curves.

## List of acronyms

AFR – Amplitude-Frequency Response.
AF – apparatus function
B(A) – XRD –Expensive (B), Cheap (A) X-ray diffractometer.
GPS – the generalized Prony's spectrum
IM – intermediate model.
LLSM – linear least square method.
PSGD – positionally-sensitive gas detector.
QP – process – Quasi-Periodic process.
XRT – X-ray tube.

*Acknowledgements: The authors labeled under scripts a) want to express their acknowledgments to the Russian Government Program of Competitive Growth of Kazan Federal University. This paper is stimulated by the R&D project realized in the frame of the JNU-KNRTU(KAI) Joint Laboratory of "Information Science and Fractal Signal Processing".*

## References

1. NIGMATULLIN, R.R., KHAMZIN, A.A., TENREIRO MACHADO, J., Physica Scripta **89**, 2014, 015201.
2. NIGMATULLIN, R.R., OSOKIN, S.I., BALEANU, D., AL-AMRI,S., AZAM,A,. MEMIC, A., The First Observation of Memory Effects in the InfraRed (FT-IR) Measurements: Do Successive Measurements Remember Each Other? PLoS ONE, **9** (4) , 2014, e94305.
3. NIGMATULLINM R.R., RAKHMATULLIN, R. Detection of quasi-periodic processes in repeated-measurements: New approach for the fitting and clusterization of different data. Communications of Nonlinear Science and Numerical Simulation **19**, 2014, p.4080.
4. NIGMATULLIN, R.R., RAKHMATULLIN, R.M., OSOKIN, S.I., How to reduce reproducible measurements to an ideal experiment? Magnetic Resonance in Solids, (Electronic Journal), **16** (2) 1, 2014, (http:// mrsej.kpfu.ru).
5. NIGMATULLIN, R.R., ZHANG, W., STICCOLI, D., General theory of experiment containing reproducible data: The reduction to an ideal" experiment, Communications in Nonlinear Science and Numerical Simulations (accepted for publication) 2015.
6. NIGMATULLIN, R.R., BUDNIKOV,H. K., A. S. STRELNIKOV, A.S., New approach for voltammetry near limit of detection: Integrated voltammograms and reduction of measurements to an "ideal" experiment Electroanalysis (accepted for publication), 2015.
7. NIGMATULLIN, R. R., TENREIRO MACHADO. J., MENEZES, R. Central European J. of Physics. **11**(6), 2013, p. 724.
8. KWAPIEN, J., DROZDZ, S., Physics Reports. **515**, 2012, p.115.
9. NIGMATULLIN, R. R., Physics of Wave Phenomena. **16**, 2008, p.119.
10. OSBORNE, M. R. ,SMYTH, G. K., SIAM Journal of Scientific and Statistical Computing. **12**, 1991, p.362.
11. KAHN, M., MACKISACK, M. S., OSBORNE, M. R. , SMYTH, G.K., Journal of Computational and Graphical Statistics, **1**, 1992, p.329.
12. OSBORNE, M. R. , SMYTH, G. K., SIAM Journal of Scientific and Statistical Computing **16**,1995, p 119

Manuscript received: 23.03.2015